Naval Research Laboratory
Washington, DC 20375-5320

NRL/MR/6790--95-7672

Theory and Group Velocity of Ultrashort, Tightly-Focused Laser Pulses

E. Esarey
P. Sprangle
J. Krall

Beam Physics Branch
Plasma Physics Division

M. Pilloff

Department of Physics
Cornell University, Ithaca, NY

June 7, 1995

REPORT DOCUMENTATION PAGE

Form Approved
OMB No. 0704-0188

1. AGENCY USE ONLY (*Leave Blank*)	2. REPORT DATE	3. REPORT TYPE AND DATES COVERED
	June 7, 1995	Interim

4. TITLE AND SUBTITLE

Theory and Group Velocity of Ultrashort, Tightly-Focused Laser Pulses

5. FUNDING NUMBERS

DOE-AI05-83ER40117
67-2005-0-3

6. AUTHOR(S)

E. Esarey, P. Sprangle, M. Pilloff*, and J. Krall

7. PERFORMING ORGANIZATION NAME(S) AND ADDRESS(ES)

Naval Research Laboratory
Washington, DC 20375-5320

8. PERFORMING ORGANIZATION REPORT NUMBER

NRL/MR/6790--95-7672

9. SPONSORING/MONITORING AGENCY NAME(S) AND ADDRESS(ES)

Office of Naval Research
800 North Quincy Street
Arlington, VA 22217-5660

Department of Energy
Washington, DC 20545

10. SPONSORING/MONITORING AGENCY REPORT NUMBER

11. SUPPLEMENTARY NOTES

*Department of Physics, Cornell University, Ithaca, NY 14843

12a. DISTRIBUTION/AVAILABILITY STATEMENT

Approved for public release; distribution unlimited.

12b. DISTRIBUTION CODE

13. ABSTRACT (*Maximum 200 words*)

The wave equation describing an ultrashort, tightly focused laser pulse in vacuum is solved analytically. Plasma dispersive effects are also included. Based on exact short-pulse solutions, analytic expressions are obtained for pulse length evolution, pulse centroid motion and group velocity. Approximate short pulse solutions are obtained to arbitrary order in the parameter $\lambda/2\pi L < 1$, where λ is the pulse wavelength and L is the length of the pulse envelope. Comparisons are made to the solutions of the paraxial wave equation and to numerical solutions of the full wave equation. The exact analytic expression for the pulse group velocity v_g, which is correctly determined from the motion of the pulse centroid, is in excellent agreement with the numerical solution. In vacuum, $1 - v_g/c = (\lambda/2\pi r_0)^2$, where r_0 is the laser spotsize at focus. Estimates for the quantity $1 - v_g/c$, based on the paraxial wave equation, are found to be in error by factor of two.

14. SUBJECT TERMS

Group velocity
Short pulse
Laser

15. NUMBER OF PAGES

24

16. PRICE CODE

17. SECURITY CLASSIFICATION OF REPORT	18. SECURITY CLASSIFICATION OF THIS PAGE	19. SECURITY CLASSIFICATION OF ABSTRACT	20. LIMITATION OF ABSTRACT
UNCLASSIFIED	UNCLASSIFIED	UNCLASSIFIED	UL

CONTENTS

THEORY AND GROUP VELOCITY OF ULTRASHORT, TIGHTLY-FOCUSED LASER PULSES

1. INTRODUCTION

Much recent interest has arisen in the study of ultrashort, high–intensity laser pulses. Numerous experiments are underway on applications of ultra–intense pulses, including particle acceleration [1-3], x–ray sources [4-7], laser fusion [8] and the study of ultrafast phenomena [9]. This activity is largely a result of the development of compact solid-state lasers based on chirped pulse amplification [10], which are capable of producing ultrahigh intensities ($\gtrsim 10^{18}$ W/cm^2) and ultrashort pulse lengths ($\lesssim 100$ fs). In order to analyze short pulse phenomena and applications, it is necessary to have accurate analytic expressions describing the properties of ultrashort, tightly focused laser pulses. For example, it may be possible to focus an intense, short laser pulse onto a group of electrons (or a diffuse plasma or gas) such that the electrons are picked up and accelerated by the laser pulse. Electron acceleration can be a result of the axial ponderomotive force associated with the fast rise in the laser intensity. Whether or not the electrons are trapped and efficiently accelerated by the laser pulse depends on the pulse profile and is a sensitive function of the pulse group velocity. Accurate expressions for the pulse envelope evolution and, in particular, the group velocity are necessary to evaluate such processes.

A common approach to the study of laser pulses is to make use of the paraxial wave equation, for which there are well–known analytical solutions [11-13]. Strictly speaking, these solutions are valid only for long laser beams: $L \gg Z_R$, where L is the characteristic length for axial variations in the pulse envelope (typically on the order of the pulse length), $Z_R = \pi r_0^2/\lambda$ is the Rayleigh length (or diffraction length), r_0 is the minimum spotsize of the pulse at focus and λ is the laser wavelength. Frequently, however, the paraxial solutions are modified and used to model short laser pulses. This can be done by multiplying the paraxial solutions by an axial profile function of the form $f(z-v_e t)$, where z is the distance along the axis of propagation, v_e is the velocity of the envelope and $f/|\partial f/\partial z| \sim L$. These modified paraxial solutions may not be accurate for very short laser pulses ($L < Z_R$).

Furthermore, it is not clear what value of v_e to use in the modified paraxial solutions. It is also not clear how the envelope velocity v_e is related to the group velocity of the pulse centroid v_g. Accurate expressions for v_g are not known. Intuitively, a laser pulse passing

Manuscript approved March 30, 1995.

through focus has $v_g < c$. In the paraxial approximation, the laser spotsize r_s evolves according to $r_s = r_0(1+z^2/Z_R^2)^{1/2}$. This implies that the laser pulse photons are traveling at the diffraction angle $\theta_d = r_0/Z_R$ with respect to the z axis. The axial component of the photon velocity is then $v_e \simeq c\cos\theta_d \simeq c(1-\theta_d^2/2)$. A similar result is obtained by analyzing the phase of the paraxial solutions. In either case, $1 - v_e/c \simeq \theta_d^2/2$. The results below indicate that this value differs from the group velocity of the pulse centroid v_g by a factor of two.

In this paper, analytic solutions to the wave equation [see Eq. (1) below] describing ultrashort, tightly focused laser pulses are found to arbitrary order in the parameter $\lambda/2\pi L < 1$. In addition, exact expressions which describe several properties of short pulses are derived, such as global conservation, pulse length evolution, centroid motion and the pulse group velocity. For example, to leading order, the laser spotsize evolves according to $r_s = r_0(1+\eta^2/Z_R^2)^{1/2}$, where $\eta = (z+ct)/2$ and the initial conditions are chosen such that the minimum spotsize r_0 occurs at the focal point $z = 0$ and $t = 0$. Hence, for a fixed time, the spotsize varies throughout the pulse. Furthermore, the pulse group velocity in vacuum, based on the motion of the pulse centroid, is given by $1 - v_g/c \simeq \theta_d^2/4$, to leading order. Detailed comparisons are made between the analytic solutions and numerical solutions to the full wave equation. The short pulse solutions discussed in this paper are limited to profiles which are Gaussian in the transverse direction, i.e., the laser field amplitude is proportional to $\exp(-r^2/r_s^2)$, where r is the radial coordinate. Generalization of the results below to describe higher order Hermite–Gaussian transverse profiles is straightforward.

The wave equation describing the three–dimensional (3D) evolution of of a laser pulse in a fully ionized plasma is given by

$$\left(\nabla^2 - \frac{1}{c^2}\frac{\partial^2}{\partial t^2}\right)\mathbf{a} = k_p^2\mathbf{a}, \tag{1}$$

where $\mathbf{a} = e\mathbf{A}_\perp/m_e c^2$ is the normalized transverse vector potential of the laser pulse (the transverse electric field is given by $e\mathbf{E}_\perp = -m_e c\partial\mathbf{a}/\partial t$) and k_p is the effective plasma wavenumber. In general, k_p is a highly nonlinear function of $\mathbf{a}$ [3]. The present study, however, will be limited to a linear plasma response where $k_p = \omega_p/c$ is constant, which is valid when $a^2 \ll 1$, where $\omega_p = (4\pi e^2 n_0/m_e)^{1/2}$ is the plasma frequency and n_0 is

the ambient electron plasma density (assumed to be uniform). Here, a^2 is related to the intensity of a linearly polarized laser field by $a^2 \simeq 0.72 \times 10^{-18}\lambda^2 I$, where λ is the laser wavelength in μm and I is the laser intensity in W/cm^2. In the $a^2 \ll 1$ limit (i.e., $I \ll 10^{18}$ W/cm^2 for $\lambda \simeq 1$ μm), the k_p^2 term models the dispersive effects of the plasma electrons. The vacuum limit corresponds to $k_p = 0$. Equation (1) indicates that the initial polarization of the laser field remains unchanged as it propagates. The axial component of the field can be found by requiring $\nabla \cdot \mathbf{E} = 0$.

The majority of previous theoretical studies of tightly focused pulse propagation has been concerned with solutions to the paraxial wave equation [11-13]. Paraxial solutions are discussed in detail in Sec. 2. I.P. Christov [14] found analytical solutions describing pulse evolution which are valid only far from focus, $z \gg Z_R$. Furthermore, the group velocity of the pulse was not considered. More recently, Horvath and Bor [15] described pulse distortions which arise when a pulse is focused by a lens with a frequency dependent index of refraction. These distortions are due to the longitudinal chromatic aberration of the lens, i.e., the focal length of the lens is a function of frequency. A short pulse of length L has a finite bandwidth $\Delta\omega \sim 1/L$. Hence, the different frequency components focus along different paths which distorts the pulse profile. Pulse distortions due to lens aberrations will be neglected in the following.

The remainder of this paper is organized as follows. Section 2 discusses solutions to the paraxial wave equation and their shortcomings. Section 3 describes the formalism for obtaining short pulse solutions to the full wave equation. Use is made of the independent variables $\zeta = z - ct$ and $\eta = (z + ct)/2$. The wave equation for the pulse envelope $\hat{a}(r, \eta, \zeta)$ is solved by taking a Fourier transform with respect to ζ, where $\mathbf{a}$ is given by the real part of $\hat{a}\exp(ik_0\zeta)\mathbf{e}_x$, with $k_0 = 2\pi/\lambda$. Several exact properties of short pulses are derived, including global conservation, pulse centroid motion and group velocity, and pulse length evolution. Section 4 presents approximate short pulse solutions based on the expansion parameter $1/k_0L < 1$. The zeroth, first, second and fourth order solutions are highlighted. Comparisons between the analytic solutions and numerical solutions to the wave equation are presented in Sec. 5. The paper concludes with a discussion in Sec. 6.

2. PARAXIAL SOLUTIONS

The mostly commonly used expressions describing the evolution of laser pulses are the solutions to the paraxial wave equation [11-13]. The paraxial wave equation can be obtained as follows. Consider a long laser pulse, i.e., a laser "beam", of the form $\mathbf{a} = \hat{a}(r,z)\exp\left[ik_0(z-ct)\right]\mathbf{e}_x$, where $\hat{a}(r,z)$ is the laser envelope and ck_0 is the laser frequency. The wave equation describing the laser envelope is given by

$$\left(\nabla_\perp^2 + 2ik_0\frac{\partial}{\partial z} + \frac{\partial^2}{\partial z^2} - k_p^2\right)\hat{a} = 0. \tag{2a}$$

The paraxial approximation involves neglecting the $\partial^2/\partial z^2$ term, which assumes a sufficiently slowly varying envelope, $|\partial\hat{a}/\partial z| \ll |k_0\hat{a}|$. The paraxial wave equation is

$$\left(\nabla_\perp^2 + 2ik_0\frac{\partial}{\partial z} - k_p^2\right)\hat{a} = 0. \tag{2b}$$

Solutions to the paraxial wave equation are well–known in terms of Hermite–Gaussian modes [11-13]. For example, the lowest order Gaussian mode is given by $\hat{a} \equiv \hat{a}_p(r,k_0,z)$, where $\hat{a}_p = a_0\exp(\psi_p)$ and

$$\psi_p(r,k_0,z) = -\frac{1}{2}\ln(1+\alpha_z^2) - \frac{r^2/r_0^2}{1+i\alpha_z} - i\tan^{-1}\alpha_z - \frac{i}{4}k_p^2r_0^2\alpha_z. \tag{3}$$

In Eq. (3), $\alpha_z = z/Z_R$, $Z_R = k_0r_0^2/2$ is the Rayleigh length, a_0 is the peak amplitude at focus, and r_0 is the minimum laser spotsize at focus. For simplicity, the focal point is chosen to be at $z = 0$. The properties of the paraxial solutions are well–known [11-13]. For example, $|\hat{a}_p| = (a_0r_0/r_s)\exp(-r^2/r_s^2)$, where $r_s = r_0(1+z^2/Z_R^2)^{1/2}$ is the laser spotsize. The paraxial solution $a_p = \hat{a}_p\exp\left[ik_0(z-ct)\right]$ can be written as

$$a_p(r,z,t) = (a_0r_0/r_s)\exp(-r^2/r_s^2 + i\phi_p), \tag{4a}$$

$$\phi_p(r,z,t) = k_0(z-ct) + \alpha_zr^2/r_s^2 - \tan^{-1}\alpha_z - k_p^2r_0^2\alpha_z/4, \tag{4b}$$

where $\phi_p = [\psi_p]_i + k_0(z-ct)$ is the total phase (the subscript i denotes the imaginary part). The effective pulse frequency ω and axial wavenumber k_z can be defined in terms of the total phase, $\omega \equiv -\partial\phi_p/\partial t$ and $k_z \equiv \partial\phi_p/\partial z$. This gives $\omega = ck_0$ and

$$k_z = k_0 - \frac{k_p^2}{2k_0} - \frac{2}{k_0r_s^2}\left[1 - \frac{r^2}{r_s^2}(1-\alpha_z)\right]. \tag{5}$$

The paraxial approximation implicitly assumes $k_p^2/k_0^2 \ll 1$ and $k_0^2 r_s^2 \gg 1$.

It is reasonable to assume that if the laser pulse length L is sufficiently long, $L \gg Z_R \gg \lambda$, where $\lambda = 2\pi/k_0$ is the laser wavelength, then the pulse can be adequately described by a paraxial solution of the form

$$a(r, z, t) = f(z - v_e t) a_p(r, z, t) \tag{6}$$

Here, the function f describes the axial profile of the pulse envelope, which is assumed to travel at the envelope velocity v_e, and $f/|\partial f/\partial z| \sim L$. It is not clear, however, what value of v_e to use in the axial profile $f(z - v_e t)$. Within the paraxial approximation, the "group velocity" of the pulse envelope v_e can be estimated from the total phase ϕ_p of the laser field. In terms of the frequency $\omega = ck_0$ and axial wavenumber k_z, Eq. (5), the effective phase velocity v_p and "group" velocities v_e are given by $v_p = \omega/k_z$ and $v_e = (\partial k_z/\partial\omega)^{-1}$. Specifically, $v_e/c = (1 + \epsilon_p)^{-1} \simeq 1 - \epsilon_p$, or

$$\frac{v_e(r,z)}{c} \simeq 1 - \frac{k_p^2}{2k_0^2} - \frac{2}{k_0^2 r_0^2}\left[\frac{(1-\alpha_z^2)}{(1+\alpha_z^2)^2} - \frac{r^2}{r_0^2}\frac{(1-6\alpha_z^2+\alpha_z^4)}{(1+\alpha_z^2)^3}\right]. \tag{7}$$

In particular, in vacuum $k_p = 0$ and at $r = z = 0$, $v_e/c \simeq 1 - 2/k_0^2 r_0^2$. Note however, that this expression for v_e is problematic, since it implies that there are regions in (r, z) for which $\epsilon_p < 0$ and $v_e > c$. To provide an accurate description of the group velocity, it is necessary to consider the motion of the pulse centroid, as is discussed below.

3. EXACT DESCRIPTION OF SHORT PULSES

To describe the behavior of short pulses, it is convenient to introduce the variables $\zeta = z - ct$ and $\eta = (z + ct)/2$. In these variables, the wave equation becomes

$$\left(\nabla_\perp^2 + 2\frac{\partial^2}{\partial\eta\partial\zeta} - k_p^2\right)\mathbf{a} = 0. \tag{8}$$

Short pulse solutions will be sought of the form $\mathbf{a} = [\hat{a}\exp(ik_0\zeta) + c.c.]\,\mathbf{e}_x/2$, where $\hat{a}(r, \zeta, \eta)$ is the laser envelope, k_0 is a constant and represents the fundamental laser pulse wavenumber, $\mathbf{e}_x$ is a unit vector in the direction of the polarization and *c.c.* denotes the complex conjugate. Using this form, the laser pulse propagates in the positive z direction,

ζ is constant for a point moving at the speed of light and is a measure of the relative axial distance within the laser pulse, and η is the time–like coordinate which represents the axial distance traveled for a point moving at the speed of light. The wave equation describing the evolution of the envelope $\hat{a}$ is given by

$$\left[\nabla_\perp^2 + 2\Big(ik_0 + \frac{\partial}{\partial\zeta}\Big)\frac{\partial}{\partial\eta} - k_p^2\right]\hat{a}(r,\zeta,\eta) = 0. \tag{9a}$$

Taking the Fourier transform in ζ gives

$$\left[\nabla_\perp^2 + 2i\Big(k_0 + k\Big)\frac{\partial}{\partial\eta} - k_p^2\right]\hat{a}_k = 0, \tag{9b}$$

where

$$\hat{a}_k(r,k,\eta) = \frac{1}{\sqrt{2\pi}}\int_{-\infty}^{\infty} d\zeta \exp(-ik\zeta)\hat{a}(r,\zeta,\eta) \tag{9c}$$

is the Fourier transform of $\hat{a}$.

Notice that Eq. (9b) is identical to the paraxial wave equation, Eq. (2b), with $z \to \eta$ and $k_0 \to k_0 + k$. Hence, explicit solutions to Eq. (9b) can be found based on the Hermite–Gaussian solutions of the paraxial wave equation [11-13]. For example, assuming the lowest order Gaussian mode, the Fourier transform of the laser envelope is given by

$$\hat{a}_k(r,k,\eta) = f_k\hat{a}_{pk}(r,k_0+k,\eta) = a_0 f_k \exp\psi_k(r,k_0+k,\eta), \tag{10a}$$

$$\psi_k(r,k_0+k,\eta) = -\frac{1}{2}\ln(1+\alpha_k^2) - \frac{r^2/r_0^2}{1+i\alpha_k} - i\tan^{-1}\alpha_k - \frac{i}{4}k_p^2 r_0^2\alpha_k, \tag{10b}$$

$$\alpha_k = \eta/Z_{Rk}, \tag{10c}$$

$$Z_{Rk} = (k_0+k)r_0^2/2. \tag{10d}$$

Note that $\hat{a}_k(\eta=0) = f_k a_0 \exp(-r^2/r_0^2)$. Hence, f_k is the Fourier transform of the initial ($\eta = 0$) axial envelope profile $f(\zeta)$. For convenience, the focal point is chosen to occur at $\eta = 0$.

Equation (10) is a valid solution for the lowest order Gaussian mode to Eq. (9b) for all k except $k = -k_0$. Notice that $k = -k_0$ corresponds to a Fourier mode component which is axially uniform, i.e., $\partial a/\partial\zeta \to 0$, which is physically uninteresting. When $k = -k_0$, the $\partial/\partial\eta$ operator in Eq. (9b) and the quantity α_k are singular and the solution Eq. (10) breaks down. These singularities can be avoided by choosing a distribution f_k which does not

contain components at $k = -k_0$. For analytical convenience in the following calculations, an axial k spectrum will be used of the form $f_k = (1 + k/k_0)f_{Gk}$, which corresponds to $f = (1 - ik_0^{-1}\partial/\partial\zeta)f_G$, where $f_G = \exp(-\zeta^2/L^2)$ represents a Gaussian axial pulse profile with a pulse length L. Specifically, the following forms for $f(\zeta)$ and f_k will be assumed,

$$f = \left(1 + \frac{2i\zeta}{k_0 L^2}\right) \exp\left(-\frac{\zeta^2}{L^2}\right), \tag{11a}$$

$$f_k = \left(1 + \frac{k}{k_0}\right) \frac{L}{\sqrt{2}} \exp\left(-\frac{k^2 L^2}{4}\right). \tag{11b}$$

Equation (11a) implies an intensity profile $I \sim |a|^2$ at focus ($\eta = 0$) given by

$$I = I_0 \left[1 + \frac{4(z - ct)^2}{k_0^2 L^4}\right] \exp\left[-\frac{2(z - ct)^2}{L^2} - \frac{2r^2}{r_0^2}\right], \tag{12}$$

where I_0 is the intensity of the pulse center at focus (at focus, the pulse center is given by $\zeta = z - ct = 0$ and $r = 0$). This represents a slightly distorted Gaussian profile, since $1/k_0^2 L^2 \ll 1$.

3.1. Global Conservation

Based on the wave equation for the pulse envelope $\hat{a}(r, \zeta, \eta)$, Eq. (9a), it is straightforward to show that the quantity

$$W \equiv \int_0^\infty dr r \int_{-\infty}^\infty d\zeta \left| \left(ik_0 + \frac{\partial}{\partial\zeta}\right) \hat{a} \right|^2, \tag{13}$$

is an exact constant of the motion, i.e., $\partial W/\partial\eta = 0$. Physically, W may be interpreted as the leading order contribution to the total pulse energy at a given η, i.e., the energy density integrated over the transverse and axial coordinates. In normalized units, the leading order components of the the transverse electric and magnetic fields are $E_x = c^{-1}\partial a/\partial t = (\partial/\partial\zeta - \frac{1}{2}\partial/\partial\eta)a$ and $B_y \simeq \partial a/\partial z = (\partial/\partial\zeta + \frac{1}{2}\partial/\partial\eta)a$. Hence,

$$E^2 + B^2 \sim |\partial a/\partial\zeta|^2 + |\partial a/\partial\eta|^2/4 \simeq |\partial a/\partial\zeta|^2 \rightarrow |(ik_0 + \partial/\partial\zeta)\hat{a}|^2,$$

which assumes $|\partial a/\partial\zeta|^2 \gg |\partial a/\partial\eta|^2, |\partial a/\partial x|^2$.

Letting $b \equiv (ik_0 + \partial/\partial\zeta)\hat{a}$ and letting $b_k = i(k_0 + k)\hat{a}_k$ denote the Fourier transform of b, W can be evaluated using the identity $\int d\zeta |b|^2 = \int dk |b_k|^2$. One finds

$$W = \frac{a_0^2 r_0^2}{4} \int_{-\infty}^\infty dk (k_0 + k)^2 |f_k|^2, \tag{14}$$

where use has been made of the fact that $\int drr|a_{pk}|^2 = a_0^2 r_0^2/4$. For the specific form of f_k given by Eq. (11),

$$W = \frac{\sqrt{2\pi}}{8} L a_0^2 r_0^2 k_0^2 \left(1 + \frac{6}{k_0^2 L^2} + \frac{3}{k_0^4 L^4}\right), \tag{15}$$

where, typically, $k_0^2 L^2 = (2\pi L/\lambda)^2 \gg 1$

3.2. Pulse Centroid and Group Velocity

Since $|b|^2$ is a globally conserved quantity, it can be used as a weight function for defining the centroid $\bar{\zeta}$ of the laser pulse, i.e.,

$$\bar{\zeta}(\eta) \equiv \langle \zeta \rangle = \int_0^\infty drr \int_{-\infty}^\infty d\zeta \zeta |b|^2 / W. \tag{16}$$

The centroid can be calculated explicitly using the relation $\int d\zeta g b = \int dk g_k b_k^*$, where $g = \zeta b$ with its transform $g_k = i\partial b_k/\partial k$ and b^* represents the complex conjugate of b. Assuming f_k to be real gives

$$\begin{aligned} \bar{\zeta} &= -\frac{1}{W} \int_0^\infty drr \int_{-\infty}^\infty dk (k_0 + k)^2 |\hat{a}_k|^2 \frac{\partial}{\partial k} \mathrm{Im}(\psi_k) \\ &= -\frac{\eta a_0^2}{4W} \left(1 + \frac{k_p^2 r_0^2}{2}\right) \int_{-\infty}^\infty dk f_k^2. \end{aligned} \tag{17}$$

For the specific form of f_k given by Eq. (11),

$$\bar{\zeta} = -\frac{\eta(1 + k_p^2 r_0^2/2)(1 + 1/k_0^2 L^2)}{k_0^2 r_0^2 (1 + 6/k_0^2 L^2 + 3/k_0^4 L^4)} \equiv -\epsilon\eta. \tag{18a}$$

Note that if a pure Gaussian axial profile $f_G = \exp(-\zeta^2/L^2)$ was used in Eqs. (14) and (17) instead of the modified Gaussian profile of Eq. (11a), this would result in corrects of order $1/k_0^2 L^2$ or higher. Specifically, the factor $(1 + 6/k_0^2 L^2 + 3/k_0^4 L^4)$ appearing in Eq. (15) and would be replaced by $(1 + 2/k_0^2 L^2)$ and Eq. (18a) would become

$$\bar{\zeta} = -\frac{\eta(1 + k_p^2 r_0^2/2)}{k_0^2 r_0^2 (1 + 2/k_0^2 L^2)}. \tag{18b}$$

The evolution of the pulse centroid $\bar{\zeta}$ can provide a definition for the group velocity v_g of the pulse, where $v_g \equiv d\bar{z}/dt$ with $\bar{\zeta} = \bar{z} - ct$. Setting $z = \bar{z}$ in Eq. (18a) and letting $\eta = (\bar{z} + ct)/2$ gives

$$v_g/c = (1 - \epsilon/2)/(1 + \epsilon/2), \tag{19}$$

where $\epsilon = -d\bar{\zeta}/d\eta$ can be determined trivially from Eq. (18a). In the limits $\epsilon \ll 1$ and $k_0^2 L^2 \gg 1$,

$$v_g/c \simeq 1 - \epsilon \simeq 1 - \frac{1}{k_0^2 r_0^2}\left(1 + \frac{k_p^2 r_0^2}{2} - \frac{5}{k_0^2 L^2}\right). \tag{20}$$

The relativistic factor γ_g associated with v_g is $\gamma_g = (1 - v_g^2/c^2)^{-1/2} \simeq 1/\sqrt{2\epsilon}$, assuming $\epsilon \ll 1$.

3.3. Pulse Length

In a similar fashion, the evolution of the pulse length L_p can be determined by defining $L_p = (\langle\zeta^2\rangle - \langle\zeta\rangle^2)^{1/2}$, where

$$\langle\zeta^2\rangle = \int_0^\infty dr r \int_{-\infty}^\infty d\zeta \zeta^2 |b|^2 / W. \tag{21}$$

Noting that $\int d\zeta g^* g = \int dk g_k^* g_k$ and assuming f_k real gives

$$\begin{aligned}\langle\zeta^2\rangle &= \int_0^\infty dr r \int_{-\infty}^\infty dk (k_0+k)^2 \frac{|a_{pk}|^2}{W}\left[\left(\frac{\partial f_k}{\partial k}\right)^2 + f_k^2\left|\frac{\partial \psi_k}{\partial k}\right|^2 + \left(\frac{\partial f_k^2}{\partial k}\right)\mathrm{Re}\left(\frac{\partial \psi_k}{\partial k}\right)\right] \\ &= \frac{a_0^2 r_0^2}{4W}\int_{-\infty}^\infty dk \left[(k_0+k)^2\left(\frac{\partial f_k}{\partial k}\right)^2 + \frac{2 f_k^2 \eta^2}{(k_0+k)^2 r_0^4}\left(1 + \frac{k_p^2 r_0^2}{2} + \frac{k_p^4 r_0^4}{8}\right)\right].\end{aligned} \tag{22}$$

For the specific form of f_k given by Eq. (11),

$$\langle\zeta^2\rangle = \frac{L^2}{4}\left[1 + \frac{10}{k_0^2 L^2} + \frac{7}{k_0^4 L^4} + \frac{2\eta^2/Z_R^2}{k_0^2 L^2}\left(1 + \frac{k_p^2 r_0^2}{2} + \frac{k_p^4 r_0^4}{8}\right)\right]\left(1 + \frac{6}{k_0^2 L^2} + \frac{3}{k_0^4 L^4}\right)^{-1}. \tag{23}$$

In the limit $k_0^2 L^2 \gg 1$ and $k_p r_0^2 \ll 1$,

$$L_p^2 \simeq \frac{L^2}{4}\left[1 + \frac{4}{k_0^2 L^2} + \frac{\eta^2/Z_R^2}{k_0^2 L^2}\left(1 - \frac{2}{k_0^2 L^2}\right)\right]. \tag{24}$$

Hence, the pulse length slowly increases as the pulse moves away from the focal point $\eta = 0$. In particular, $L_p(\eta)/L_p(0) \simeq 1 + \eta^2/\left[8 Z_R^2 k_0^2 L_p^2(0)\right]$, assuming $k_0^2 L^2 \gg 1$.

4. APPROXIMATE SOLUTIONS

The laser pulse envelope $\hat{a}(r, \zeta, \eta)$ is given by the inverse transform of Eq. (10),

$$\hat{a}(r, \zeta, \eta) = \frac{1}{\sqrt{2\pi}}\int_{-\infty}^\infty dk \exp(ik\zeta) f_k a_0 \exp(\psi_k). \tag{25}$$

For a particular choice of f_k, it is unlikely that exact analytical solutions can be obtained for the inverse transform Eq. (25). Physically, k represents the transform of the ζ variations which occur in the laser envelope. Typically, $k \sim 1/L$ and $k/k_0 \sim 1/k_0 L \ll 1$. Hence, the function $\psi_k(k_0 + k)$ can be expanded about k_0 and approximate expressions for the inverse transform can be obtained, i.e.,

$$\psi_k(r, k_0 + k, \eta) = \psi(k_0) + \frac{\partial \psi}{\partial k_0} k + \frac{1}{2} \frac{\partial^2 \psi}{\partial k_0^2} k^2 + \cdots, \tag{26a}$$

where

$$\psi(k_0) = -\frac{1}{2} \ln(1 + \alpha^2) - \frac{r^2/r_0^2}{1 + i\alpha} - i \tan^{-1} \alpha - \frac{i}{4} k_p^2 r_0^2 \alpha, \tag{26b}$$

$$\frac{\partial \psi}{\partial k_0} = \frac{i\alpha}{k_0} \left[\frac{1}{1 + i\alpha} - \frac{r^2/r_0^2}{(1 + i\alpha)^2} + \frac{k_p^2 r_0^2}{4} \right], \tag{26c}$$

$$\frac{\partial^2 \psi}{\partial k_0^2} = -\frac{i\alpha}{k_0^2} \left[\frac{2 + i\alpha}{(1 + i\alpha)^2} - \frac{2r^2/r_0^2}{(1 + i\alpha)^3} + \frac{k_p^2 r_0^2}{2} \right], \tag{26d}$$

and $\alpha = \eta / Z_R$.

4.1. Zeroth Order Solution

To lowest order, $\psi_k \simeq \psi(k_0)$, independent of k. The inverse transform Eq. (25) gives the zeroth order solution

$$\hat{a}^{(0)}(r, \zeta, \eta) = a_0 f(\zeta) \exp(\psi). \tag{27}$$

The zeroth order solution is similar to the paraxial solution, Eq. (6), with the independent variable z replaced by $\eta = (z + ct)/2$. Furthermore, to zeroth order, the axial profile is $f(\zeta) = f(z - ct)$, i.e., the envelope propagates with $v_g = c$. Notice that the initial ($t = 0$) envelope is given by $\hat{a}(t = 0) = a_0 f(z) \exp[\psi(z/2)]$, in contrast to the paraxial solution, for which $\hat{a}_p(t = 0) = a_0 f(z) \exp[\psi(z)]$.

The full zeroth order solution $a^{(0)} = \hat{a}^{(0)} \exp(ik_0 \zeta)$ can be written as

$$a^{(0)} = a_0 \frac{r_0}{r_s} \left(1 + \frac{2i\zeta}{k_0 L^2} \right) \exp\left(-\frac{r^2}{r_s^2} - \frac{\zeta^2}{L^2} + i\phi^{(0)} \right), \tag{28a}$$

$$\phi^{(0)} = k_0 \zeta + \alpha r^2 / r_s^2 - \tan^{-1} \alpha - k_p^2 r_0^2 \alpha / 4, \tag{28b}$$

where $\phi^{(0)} = \psi_i + k_0\zeta$ is the total phase of the zeroth order solution and $r_s = r_0(1+\alpha^2)^{1/2}$ is the spotsize. The effective pulse frequency $\omega^{(0)}$ and axial wavenumber $k_z^{(0)}$ of the zeroth order solution can be defined by $\omega^{(0)} \equiv -\partial\phi^{(0)}/\partial t$ and $k_z^{(0)} \equiv \partial\phi^{(0)}/\partial z$. This gives

$$\omega^{(0)} = ck_0\left\{1 + \frac{k_p^2}{4k_0^2} + \frac{1}{k_0^2 r_s^2}\left[1 - \frac{r^2}{r_s^2}(1-\alpha^2)\right]\right\}, \tag{29a}$$

$$k_z^{(0)} = k_0\left\{1 - \frac{k_p^2}{4k_0^2} - \frac{1}{k_0^2 r_s^2}\left[1 - \frac{r^2}{r_s^2}(1-\alpha^2)\right]\right\}, \tag{29b}$$

Notice that Eqs. (29a) and (29b) satisfy the local dispersion relation

$$(\omega^{(0)})^2 + c^2(k_z^{(0)})^2 = c^2k_p^2 + \frac{4}{r_s^2}\left[1 - \frac{r^2}{r_s^2}(1-\alpha^2)\right]. \tag{30}$$

This is in contrast to the paraxial solution, in which the above dispersion relation is only approximately satisfied for $\omega = ck_0$ and k_z given by Eq. (5).

4.2. First Order Solution

To first order, $\psi_k \simeq \psi(k_0) + \psi' k$, where the prime denotes $\partial/\partial k_0$. The first order solution is

$$\begin{aligned}\hat{a}^{(1)}(r,\zeta,\eta) &= \frac{1}{\sqrt{2\pi}}\int_{-\infty}^{\infty} dk \exp\left[ik(\zeta - i\psi')\right] f_k a_0 \exp(\psi) \\ &= a_0 f(\zeta - i\psi')\exp(\psi).\end{aligned} \tag{31}$$

The first order solution includes corrections to the evolution of the axial profile, i.e., $f(\zeta - i\psi')$. In particular, first order group velocity effects are included. Intuitively, the local envelope velocity can be estimated by setting $d(\zeta - i\psi')_r/dt = 0$, where the subscript r denotes the real part, and by identifying $v_e = dz/dt$. This gives $v_e/c = (1-\epsilon_1/2)/(1+\epsilon_1/2)$, i.e.,

$$\frac{v_e(r,\eta)}{c} \simeq 1 - \epsilon_1 = 1 - \frac{2}{k_0^2 r_0^2}\left[\frac{(1-\alpha^2)}{(1+\alpha^2)^2} - \frac{r^2(1-6\alpha^2+\alpha^4)}{r_0^2(1+\alpha^2)^3} + \frac{k_p^2 r_0^2}{4}\right]. \tag{32}$$

where $\epsilon_1 = Z_R^{-1}\partial\psi_i'/\partial\alpha$ (the subscript i denotes the imaginary part). Alternatively, a local value of the pulse centroid $\langle\zeta\rangle_\zeta$ as a function of radius can be defined by averaging over the axial profile, i.e.,

$$\langle\zeta\rangle_\zeta = \frac{\int d\zeta\zeta|f|^2}{\int d\zeta|f|^2} = -\psi_i'(r,\alpha), \tag{33}$$

where a Gaussian axial profile was assumed, $f = \exp(-\zeta^2/L^2)$. (If the quantity $|b|^2$ is used as a weight function with f given by Eq. (11), an identical result is obtained plus corrections of order $1/k_0^2L^2$ or higher.) Equation (33) implies that $v_e/c = (1-\epsilon_1/2)/(1+\epsilon_1/2)$ as before, i.e., the local envelope velocity is given by Eq. (32).

The above discussion sheds some light on the interpretation of the paraxial result for the envelope velocity given by Eq. (7). Notice that the paraxial result is identical to Eq. (32) with $\eta \to z$ in the definition of α. Both Eqs. (7) and (32) exhibit regions in (r, α) for which $v_e > c$. Hence, neither of these expressions should be interpreted as the pulse group velocity. Instead, Eqs. (7) and (32) should be interpreted as the velocity of the local pulse centroid $\langle\zeta\rangle_\zeta$ defined at a specific radius. Note that a change in the local value of $\langle\zeta\rangle_\zeta$ at fixed r does not necessarily correspond to an axial transport of energy. Changes in $\langle\zeta\rangle_\zeta$ can reflect distortions in the pulse profile as it evolves. Consider, for example, a pulse profile which is initially symmetric and centered about the focal point such that $\langle\zeta\rangle_\zeta = 0$ at all r. As the pulse propagates, the front of the pulse expands radially (diffracts) as it moves away from the focal point. The back of the pulse, which is initially located behind the focal point, will contract radially as it moves towards the focal point. The pulse is now asymmetric, with the front of the pulse wider than the back. For sufficiently large r, this can cause the local centroid $\langle\zeta\rangle_\zeta$ to move towards the front of the pulse resulting in a "local" $v_e(r,\eta) > c$, as indicated by Eq. (32). However, this local centroid motion is associated with the distortions of the pulse profile and a radial transport of energy, not with an axial transport of energy.

It is more accurate to identify the group velocity of the pulse with the motion of the actual centroid, $\bar{\zeta}$, of the entire pulse. The pulse centroid $\bar{\zeta} = \langle\zeta\rangle$ is given by averaging over both the radial and axial profiles:

$$\bar{\zeta} = \frac{\int dr r \int d\zeta \zeta |f|^2 \exp(2\psi_r)}{\int dr r \int d\zeta |f|^2 \exp(2\psi_r)} = -\frac{\eta}{k_0^2 r_0^2}\left(1 + \frac{k_p^2 r_0^2}{2}\right) = -\epsilon_2 \eta. \tag{34}$$

To first order, Eq. (34) is equivalent to Eq. (16), producing the leading order contribution to the exact expression given by Eq. (18a). The group velocity of the centroid is then

$$v_g/c = \frac{(1-\epsilon_2/2)}{(1+\epsilon_2/2)} \simeq 1 - \frac{1}{k_0^2 r_0^2}\left(1 + \frac{k_p^2 r_0^2}{2}\right), \tag{35}$$

which is a constant independent of η.

In addition to group velocity effects, the first order solution has additional terms which affect the phase of the laser pulse. For example, the leading order correction to the total phase is given by $\phi^{(1)} = \phi^{(0)} + 2\zeta\psi_r'/L^2$, where $\phi^{(0)}$ is given by Eq. (28b). This additional term gives contributions to the effective frequency and wavenumber of the pulse. For example, the effective frequency, defined as $\omega^{(1)} = -\partial\phi^{(1)}/\partial t$, is given by $\omega^{(1)} = \omega^{(0)} + \delta\omega^{(1)}$, where $\omega^{(0)}$ is given by Eq. (29a) and

$$\frac{\delta\omega^{(1)}}{ck_0} = \frac{2}{k_0^2L^2}\left\{\frac{\alpha^2}{(1+\alpha^2)}\left(1-\frac{2r^2}{r_s^2}\right) - \frac{\zeta\alpha}{Z_R(1+\alpha^2)^2}\left[1-\frac{2r^2}{r_s^2}(1-\alpha^2)\right]\right\}. \tag{36}$$

Notice that along the axis, $r = 0$, the frequency varies slightly throughout the pulse, $\delta\omega^{(1)} = \delta\omega^{(1)}(\zeta)$, and evolves as the pulse propagates away from focus, $\delta\omega^{(1)} = \delta\omega^{(1)}(\eta)$.

4.3. Second Order Solution

For a pulse with a Gaussian axial profile, analytical expressions can be obtained for $\hat{a}$ to second order. Approximating $\psi_k = \psi + \psi' k + \psi'' k^2/2$ and using the expression for f_k given by Eq. (11) gives

$$\hat{a}^{(2)}(r,\zeta,\eta) = \frac{a_0}{\sqrt{1-2\psi''/L^2}}\left[1+\frac{2i(\zeta-i\psi')}{k_0L^2(1-2\psi''/L^2)}\right]\exp\left[\psi - \frac{(\zeta-i\psi')^2/L^2}{(1-2\psi''/L^2)}\right]. \tag{37}$$

This analytic form for the second order solution will be compared with numerical solutions to the wave equation in Sec. 5.

4.4. Solution to Arbitrary Order

Keeping the full expansion for ψ_k and expanding the second order and higher terms in the exponential gives a solution to arbitrary order,

$$\hat{a}^{(n)}(r,\zeta,\eta) = \frac{1}{\sqrt{2\pi}}\int_{-\infty}^{\infty} d\hat{k}\left(1+S+\frac{1}{2}S^2+\cdots+\frac{1}{n!}S^n\right)\exp\left[\psi + i(\zeta-i\psi')k\right], \tag{38}$$

where

$$S = \frac{1}{2}\frac{\partial^2\psi}{\partial k_0^2}k^2 + \cdots + \frac{1}{n!}\frac{\partial^n\psi}{\partial k_0^n}k^n. \tag{39}$$

Equation (38) can be readily evaluated. For example, keeping all terms up to order k^4,

$$\hat{a}^{(4)}(r,\zeta,\eta) = a_0 e^{\psi}\left[1-\frac{\psi''}{2}\frac{\partial^2}{\partial\zeta^2}+\frac{i\psi'''}{6}\frac{\partial^3}{\partial\zeta^3}+\left(\frac{\psi^{(iv)}}{24}-\frac{(\psi'')^2}{8}\right)\frac{\partial^4}{\partial\zeta^4}\right]f(\zeta-i\psi'). \tag{40}$$

5. COMPARISON TO NUMERICAL SOLUTIONS

The wave equation, Eq. (9a), can be solved numerically, using standard techniques, to obtain $\hat{a}(r, \zeta, \eta)$. For example, consider a laser pulse at the point of focus ($\eta = 0$) with

$$\hat{a}(r, \zeta, 0) = a_0 \left(1 + \frac{2i\zeta}{k_0 L^2}\right) \exp\left[-\left(\frac{r^2}{r_0^2} + \frac{\zeta^2}{L^2}\right)\right]. \tag{41}$$

The evolution of this laser pulse in vacuum, as a function of η, can be estimated using the first order solution Eq. (31) [with $f(\zeta) = (1 + 2i\zeta/k_0 L^2)\exp(-\zeta^2/L^2)$], the second order solution Eq. (37), or by numerically solving Eq. (9a) using Eq. (41) as the initial condition. The result for the second order solution is shown in Fig. 1, where the real part of $a = \hat{a}\exp(ik_0\zeta)$ is plotted versus r and ζ at fixed time ($t = \eta - \zeta/2$) for (a) $t = 0$ and (b) $t = 2Z_R/c$. In this example, $\lambda = 2.5$ μm and $L = r_0 = 5$ μm, such that $Z_R \simeq 31.4$ μm and $L/\lambda = r_0/\lambda = 2$. The curvature of the wave fronts as the laser pulse moves away from focus is clearly observable in Fig. 1(b).

The numerical solution for the parameters of Fig. 1 is compared to the first and second order solutions in Fig. 2. Here, the percentage difference $100(a^{(n)} - a^{(num)})/\mathrm{Max}(a^{(n)})$ is plotted versus r and ζ at $\eta = Z_R$ for (a) the first order solution $a^{(1)}$ and (b) the second order solution $a^{(2)}$, where $a^{(num)}$ denotes the numerical solution and $\mathrm{Max}(a^{(n)})$ denotes the maximum value of the n-th order solution $a^{(n)}$. The numerical solution agrees with the approximate solutions to better than 1%. Numerical results show that this error decreases as L/λ increases.

The group velocity of the numerical solution can be determined by numerically evaluating the pulse centroid $\bar{\zeta}$, Eq. (16), using the numerical solution in the integrand. From Eq. (19), the group velocity is given by $v_g/c = (1 - \epsilon/2)/(1 + \epsilon/2)$, where the quantity $\epsilon = -d\bar{\zeta}/d\eta$ is evaluated numerically. The result is compared to the analytical solution, Eqs. (18a) and (19), in Fig. 3, where $1 - v_g/c$ is plotted versus η for each case using the same parameters as in Fig. 1. The local envelope velocity v_e at $r = 0$ can be similarly determined from the numerical solution by integrating only over ζ on the right–hand side of Eq. (16). The result is compared to Eq. (32) in Fig. 3. The numerical results show excellent agreement with theory.

6. SUMMARY AND DISCUSSION

New solutions to the wave equation, Eq. (1), have been derived which describe an ultrashort, tightly focused laser pulse propagating through a plasma with a linear response or through vacuum. The wave equation for the pulse envelope $\hat{a}(r, \zeta, \eta)$, where $a = \hat{a}\exp(ik_0\zeta) + c.c$, was solved making use of the independent variables $\zeta = z - ct$ and $\eta = (z+ct)/2$ and by taking a Fourier transform with respect to ζ. Solutions for the transform of the envelope, $\hat{a}_k(r, k_0 + k, \eta)$, could then be found without approximation in terms of Hermite–Gaussian modes. The solutions are analogous to solutions of the paraxial wave equation. For simplicity, this study was limited to envelopes in which the radial profile is described by the fundamental Gaussian mode, i.e., $|a| \sim \exp(-r^2/r_s^2)$. Generalization to higher order Hermite–Gaussian modes should be straightforward. Letting the solution to the paraxial wave equation, Eq. (2b), be denoted by $\hat{a} = \hat{a}_p(r, k_0, z)$, the exact solution to the full wave equation for $\hat{a}_k$, Eq. (9b), is given by $\hat{a}_k = f_k\hat{a}_p(r, k_0 + k, \eta)$, as is indicated by Eq. (10), where f_k is the fourier transform of the axial pulse profile at $\eta = 0$.

Based on the exact solution for the transform of the envelope $\hat{a}_k$, several exact properties of ultrashort, tightly focused laser pulses were determined. General expressions were determined for arbitrary axial profiles, f_k, and specific expressions were determined for the case of a quasi–Gaussian axial profile given by Eq. (11).

For a pulse with a quasi–Gaussian axial profile, the quantity $W = \int drr \int d\zeta|b|^2$, where $b = (ik_0 + \partial/\partial\zeta)\hat{a}$, was identified as a globally conserved quantity of the full wave equation for the envelope, Eq. (9a), i.e., $\partial W/\partial\eta = 0$. The quantity W is roughly equivalent to the total pulse energy at fixed η. Using the quantity $|b|^2$ as a weight function, an expression for the pulse centroid $\bar{\zeta}$ was determined, Eq. (18a), by integrating ζ over the axial and radial coordinates. The motion of the centroid was used to define the group velocity of the pulse, $v_g \equiv d\bar{z}/dt$, where $\bar{\zeta} = \bar{z} - ct$. The resulting value for v_g is given by Eq. (19). By averaging ζ^2 over the axial and radial coordinates with $|b|^2$ as the weight function, an expression for the laser pulse length L_p was determined, Eq. (24). It was found that the pulse length slowly increased as the pulse propagates.

Approximate solutions to the laser pulse envelope $\hat{a}(r, \zeta, \eta)$ were found by expanding

$\hat{a}_k(r, k_0 + k, \eta)$ about k_0 for $|k/k_0| \sim 1/k_0 L \ll 1$ and evaluating the inverse transform. Approximate solutions for $\hat{a}(r, \zeta, \eta)$ were found to arbitrary order in $|k/k_0|$. The zeroth order solution, Eq. (27), gave $\hat{a}^{(0)} = f(\zeta)\hat{a}_p(r, k_0, \eta)$, where $\hat{a}_p(r, k_0, z)$ is the solution to the paraxial wave equation. This indicates that in order to describe a short pulse with the paraxial solution, the variable z should be replaced by the correct propagation variable $\eta = (z + ct)/2$. Furthermore, $|\hat{a}^{(0)}| = |f(\zeta)|(r_0/r_s)\exp(-r^2/r_s^2)$, where the spotsize is given by $r_s = r_0(1 + \eta^2/Z_R^2)^{1/2}$. To zeroth order, the envelope propagates at c, i.e., group velocity effects are not included. The first order solution is $\hat{a}^{(1)} = f(\zeta - i\psi')\hat{a}_p(r, k_0, \eta)$, as indicated by Eq. (31), where $\hat{a}_p = \exp(\psi)$ and ψ and ψ' are given by Eq. (26). The first order solution contains group velocity effects, with the group velocity, Eq. (35), in agreement with the exact expression, Eq. (19), to leading order. Higher order solutions for $\hat{a}$ contain corrections to higher order in the small parameter $1/k_0^2 L^2$.

Of fundamental importance is the group velocity of a tightly focused, ultrashort laser pulse. Solutions to the paraxial wave equation imply an envelope velocity $v_e(r, z)$ given by Eq. (7). This can not be interpreted as a group velocity, since there are regions in (r, z) for which $v_e > c$. At the focal point, $1 - v_e(0, 0)/c \simeq 2/k_0^2 r_0^2$, a value which differs from $1 - v_g/c$ by a factor of two. By analyzing the first order solution $\hat{a}^{(1)}$ to the full wave equation, the interpretation of the paraxial result $v_e(r, z)$ becomes clear. Using $\hat{a}^{(1)}$, the expression for the local pulse centroid $\langle\zeta\rangle_\zeta$, which is a function of r and η as given by Eq. (33), was determined by averaging ζ over the axial pulse profile at a fixed radius r. If the motion of the local centroid $\langle\zeta\rangle_\zeta$, which is a function of r and η, is used to define a local envelope velocity $v_e(r, \eta)$, the result, Eq. (32), is identical to the paraxial result $v_e(r, z)$ with $z \to \eta$. It clear that $v_e(r, \eta)$ is not the pulse group velocity, but instead is the velocity of the local centroid $\langle\zeta\rangle_\zeta$ at a fixed radius. The fact that regions in (r, η) exist where $v_e(r, \eta) > c$ indicates that $v_e(r, \eta)$ does not represent the axial velocity at which pulse energy is transported.

An improved definition of the pulse group velocity is given by considering the motion of the centroid $\bar{\zeta}$ of the entire pulse, Eqs. (16) and (34), which is determined by averaging ζ over both the axial and radial pulse profiles. The pulse group velocity is given by $v_g = d\bar{z}/dt$, where $\bar{\zeta} = \bar{z} - ct$. The exact expression for v_g is given by Eq. (19). In the

limits $k_0^2 r_0^2 \gg 1$ and $k_0^2 L^2 \gg 1$,

$$1 - \frac{v_g}{c} \simeq \frac{1}{k_0^2 r_0^2}\left(1 + \frac{k_p^2 r_0^2}{2} - \frac{5}{k_0^2 L^2}\right). \tag{42}$$

In addition to finite spotsize and plasma dispersive effects, the group velocity is also slightly reduced due to the finite pulse length. Notice that v_g is independent of z such that the pulse centroid propagates at a constant velocity. Thus Eq. (42) is valid both at focus and far from focus. The relativistic factor associated with the pulse group velocity, $\gamma_g = (1 - v_g^2/c^2)^{-1/2}$, to leading order, is

$$\gamma_g \simeq \sqrt{2}(\pi r_0/\lambda)\left(1 + k_p^2 r_0^2/2\right)^{-1/2}. \tag{43}$$

For a tightly focused laser pulse, γ_g can be relatively small.

As an example, consider the possibility of accelerating an electron from rest with the axial ponderomotive force of an intense, ultrashort laser pulse. For a fixed axial ponderomotive force, electron trapping is easier the lower the value of γ_g. For a laser pulse in vacuum with $r_0/\lambda = 3$, $\gamma_g \simeq 13$ and it may be possible for a sufficiently intense laser pulse to pick up and accelerate an electron from rest.

Acknowledgments

The authors acknowledge useful conversations with G. Mourou. This work was supported by the Office of Naval Research and the Department of Energy.

References

1. See, e.g., *Advanced Accelerator Concepts*, edited by J. Wurtele, AIP Conf. Proc. **279** (American Institute of Physics, New York, 1993).
2. C.E. Clayton, K.A. Marsh, A. Dyson, M. Everett, A. Lal, W.P. Leemans, R. Williams and C. Joshi, Phys. Rev. Lett. **70**, 37 (1993); C.E. Clayton, M.J. Everett, A. Lal, D. Gordon, K.A. Marsh and C. Joshi, Phys. Plasmas **1**, 1753 (1994).
3. P. Sprangle, E. Esarey, J. Krall and G. Joyce, Phys. Rev. Lett. **69**, 2200 (1992); E. Esarey, P. Sprangle, J. Krall, A. Ting, and G. Joyce, Phys. Fluids B **5**, 2690 (1993).
4. N.H. Burnett and P.B. Corkum, J. Opt. Soc. Am. **6**, 1195 (1989).
5. D.C. Eder, P. Amendt, L.B. DaSilva, R.A. London, B.J. MacGowan, D.L. Matthews, B.M. Penetrante, M.D. Rosen, S.C. Wilks, T.D. Donnelly, R.W. Falcone and G.L. Strobel, Phys. Plasmas **1**, 1744 (1994).
6. P. Sprangle, A. Ting, E. Esarey and A. Fisher, J. Appl. Phys. **72**, 5032 (1992); E. Esarey, S.K. Ride and P. Sprangle, Phys. Rev. E **48**, 3003 (1993).
7. K.J. Kim, S. Chattopadhyay and C.V. Shank, Nucl. Instr. Meths. **A341**, 351 (1994).
8. M. Tabak, J. Hammer, M.E. Glinsky, W.L. Kruer, S.C. Wilks, J. Woodworth, E.M. Campbell, M.D. Perry and R.J. Mason, Phys. Plasmas **1**, 1626 (1994).
9. See, e.g., *Ultrafast Phenomena VIII*, ed. by J.L. Martin, A. Migus, G.A. Mourou and A.H. Zewail (Springer–Verlag, Berlin, 1993).
10. D. Strickland and G. Mourou, Opt. Commun. **56**, 216 (1985); G. Mourou and D. Umstadter, Phys. Fluids B **4**, 2315 (1992); M.D. Perry and G. Mourou, Science **264**, 917 (1994).
11. P.W. Milonni and J.H. Eberly, *Lasers* (Wiley, New York, 1988), chap. 14.
12. A. Yariv, *Quantum Electronics*, third edition (Wiley, New York, 1989), chap. 6.
13. H.A. Haus, *Waves and Fields in Optoelectronics* (Prentice–Hall, Elnglewood Cliffs, NJ, 1984), chap. 5.
14. I.P. Christov, Optics Comm. **53**, 364 (1985).
15. Z.L. Horvath and Zs. Bor, Optics Comm. **108**, 333 (1994); Z.L. Horvath and Zs. Bor, Optics Comm. **100**, 6 (1993); Zs. Bor and Z.L. Horvath, Optics Comm. **94**, 249 (1992).

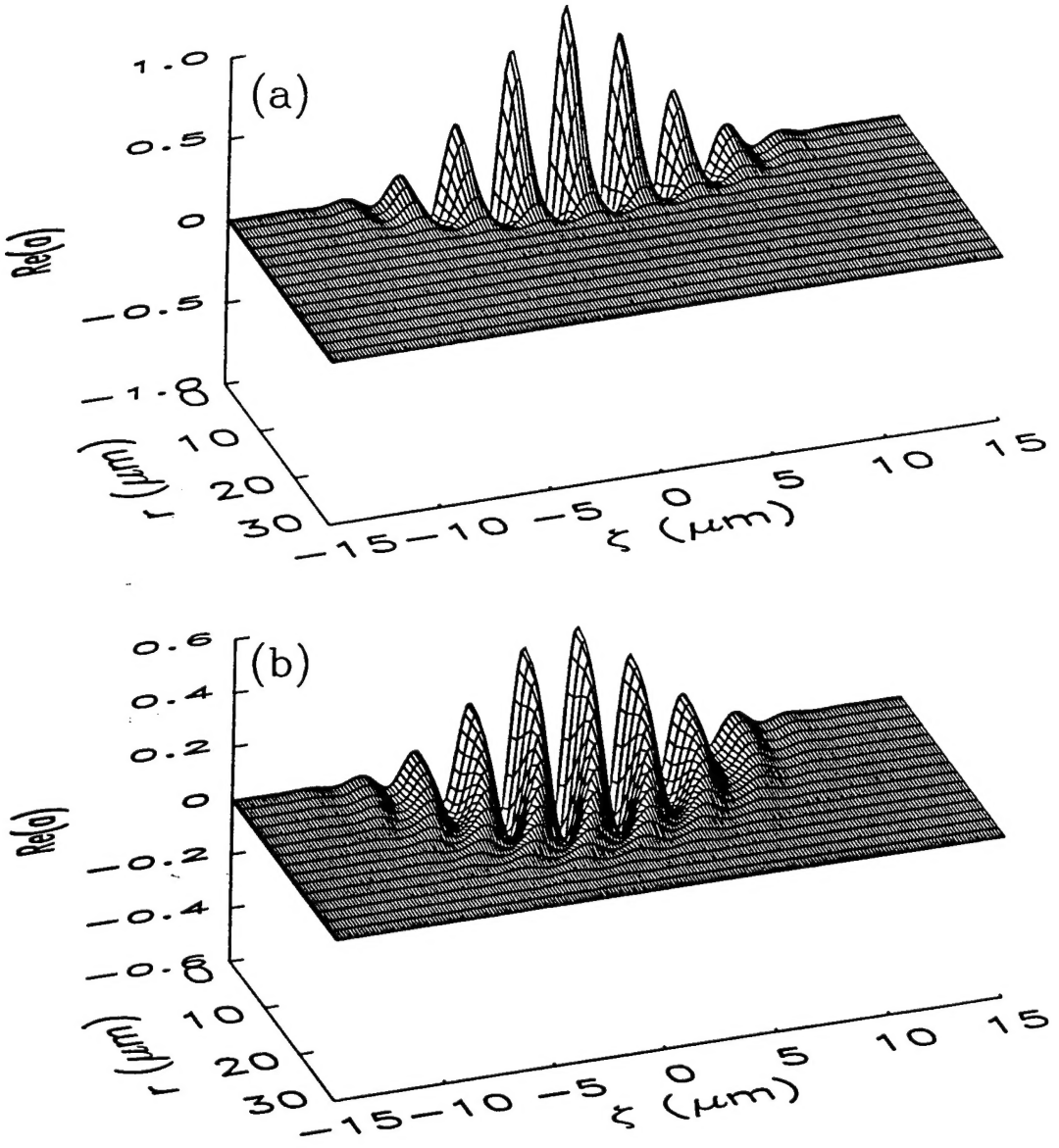

Fig. 1: Second order solution: Real part of $a = \hat{a}\exp(ik_0\zeta)$ plotted versus r and $\zeta = z - ct$ at (a) $t = 0$ and (b) $t = 2Z_R/c$ for $L/\lambda = r_0/\lambda = 2$ and $\lambda = 2.5$ μm. This shows the evolution of the normalized vector potential of the laser field for a pulse of 15 fs duration with a central wavelength of 2.5 μm. Plot (a) shows the initial laser field at $t = 0$ at the focal point where the minimum spot size is $r_0 = 5$ μm. Plot (b) shows the laser field after propagating a distance of two Rayleigh lengths from the focal point, $ct = 2Z_R \simeq 63$ μm. Notice in (b) the curvature of the wavefronts as the pulse diffracts.

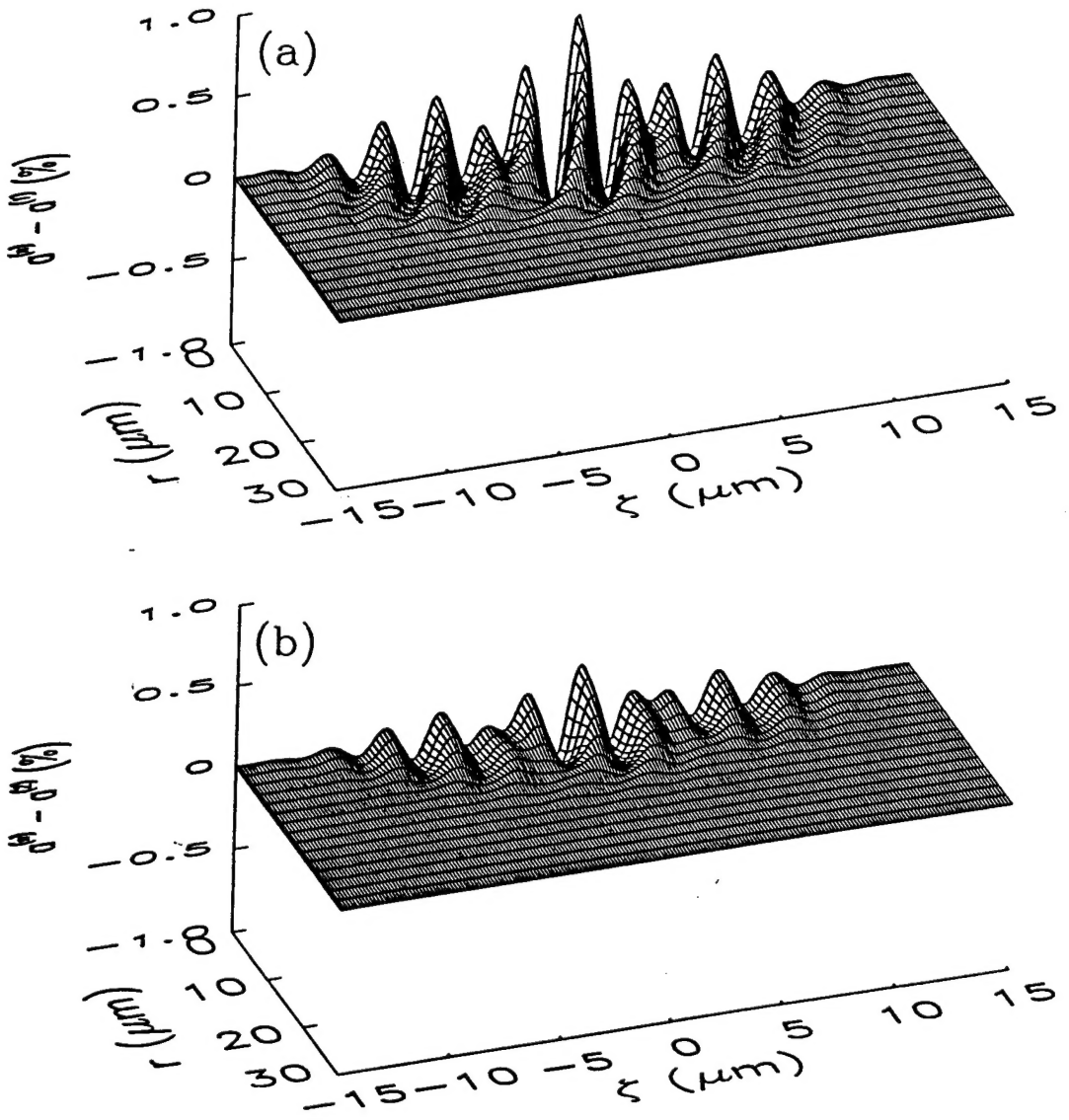

Fig. 2: Percentage difference $100(a^{(n)} - a^{(num)})/\mathrm{Max}(a^{(n)})$ between numerical solution to the wave equation $a^{(num)}$ and n-th order analytic solution $a^{(n)}$ plotted versus r and $\zeta = z - ct$ for (a) the first order solution $a^{(1)}$ and (b) the second order solution $a^{(2)}$. The parameters are $L/\lambda = r_0/\lambda = 2$ and $\lambda = 2.5$ μm and the comparisons are done after propagating a distance $\eta = (z + ct)/2 = Z_R$ from the focal point.

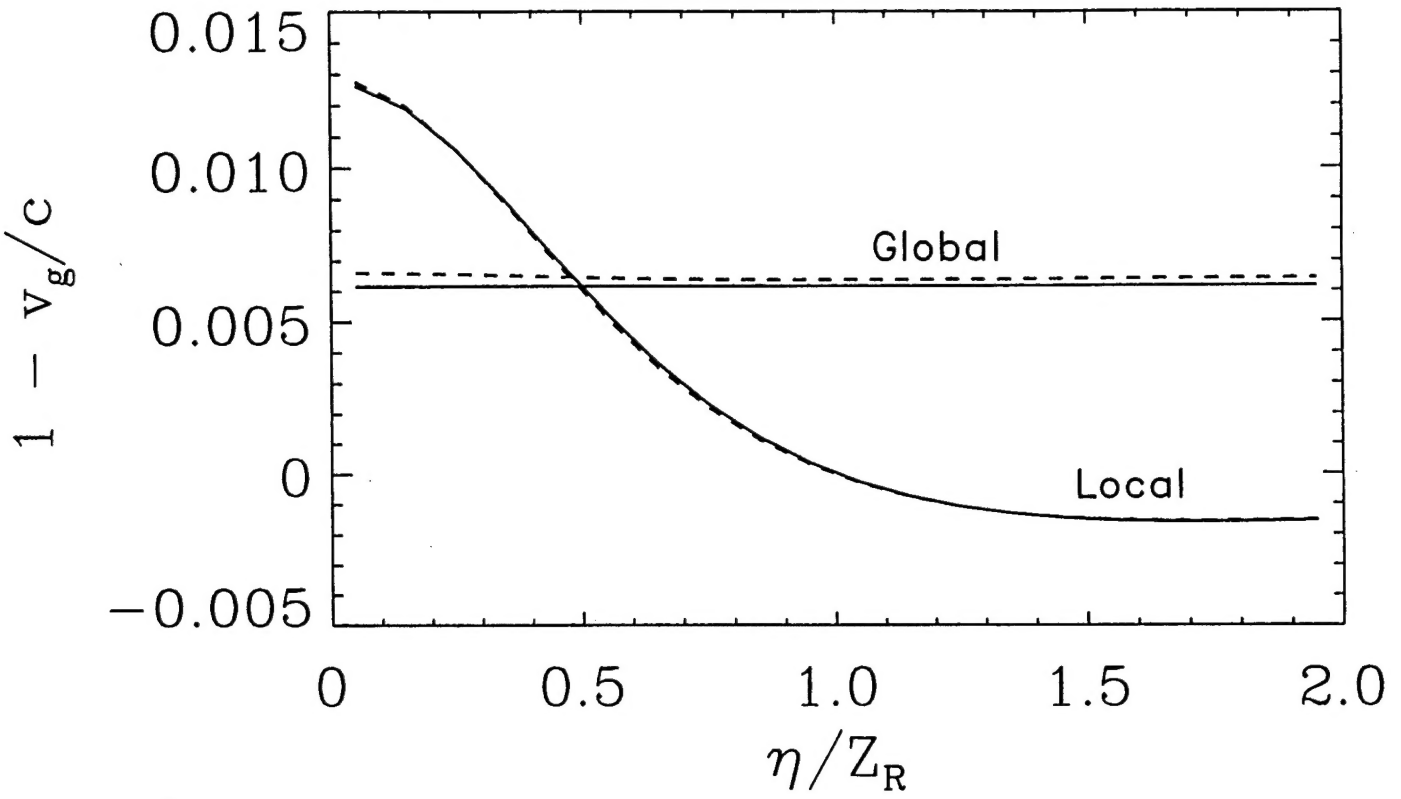

Fig. 3: Quantity $1 - v/c$ versus propagation distance $\eta = (z + ct)/2$ as given by analysis (solid) and numerical solution to the wave equation (dashed). Comparisons are done for two cases: (a) $v = v_g$, where v_g is the velocity of the pulse centroid [see Eq. (19)] and (b) $v = v_e$, where $v_e = v_e(r = 0, \eta)$ is the local envelope velocity [see Eq. (32)] evaluated along the axis $r = 0$. Here, $L/\lambda = r_0/\lambda = 2$, $\lambda = 2.5$ μm and $\eta = 0$ is the focal point.